

The Influence of Local Electric Fields on Photoinduced Absorption in Dye-Sensitized Solar Cells

Ute B. Cappel,[†] Sandra M. Feldt,[†] Jan Schöneboom,[‡] Anders Hagfeldt,[†] and Gerrit Boschloo^{*,†}

Department of Physical and Analytical Chemistry, Ångström laboratory, Uppsala University, Box 259, 751 05 Uppsala, Sweden and BASF SE, Speciality Chemicals Research, D-67056 Ludwigshafen, Germany

Received March 19, 2010; E-mail: gerrit.boschloo@fki.uu.se

Abstract: The dye-sensitized solar cell (DSC) challenges conventional photovoltaics with its potential for low-cost production and its flexibility in terms of color and design. Transient absorption spectroscopy is widely used to unravel the working mechanism of DSCs. A surprising, unexplained feature observed in these studies is an apparent bleach of the ground-state absorption of the dye, under conditions where the dye is in the ground state. Here, we demonstrate that this feature can be attributed to a change of the local electric field affecting the absorption spectrum of the dye, an effect related to the Stark effect first reported in 1913. We present a method for measuring the effect of an externally applied electric field on the absorption of dye monolayers adsorbed on flat TiO₂ substrates. The measured signal has the shape of the first derivative of the absorption spectra of the dyes and reverses sign along with the reversion of the direction of the change in dipole moment upon excitation relative to the TiO₂ surface. A very similar signal is observed in photoinduced absorption spectra of dye-sensitized TiO₂ electrodes under solar cell conditions, demonstrating that the electric field across the dye molecules changes upon illumination. This result has important implications for the analysis of transient absorption spectra of DSCs and other molecular optoelectronic devices and challenges the interpretation of many previously published results.

Introduction

In dye-sensitized solar cells (DSCs),^{1–4} dye molecules attached to a large band gap semiconductor are responsible for light absorption. Upon photoexcitation, the dye molecules inject an electron into the n-type semiconductor (most often TiO₂) and are subsequently regenerated by a redox mediator. This redox mediator usually consists of a redox couple (iodide/triiodide) in a liquid solvent containing a large concentration of ions but can also be a solid state hole conductor such as 2,2',7',7'-tetrakis-(*N,N*-di-*p*-methoxyphenyl-amine)-9,9'-spirobifluorene (spiro-MeOTAD).^{5,6} To obtain good light harvesting efficiencies, mesoporous semiconductor electrodes are used, which provide a large surface area for dye adsorption. The pores of the electrode are filled by redox electrolyte, which screens the electrons in the semiconductor, and thus there is no global electric field. Many different dye molecules have been investigated as sensitizers for DSCs. The most efficient ones are functional ruthenium(II)-polypyridyl complexes such as N3 and

N719.^{3,7} Alternatively, cheaper, metal-free organic dyes of a donor–acceptor type are used. These can be tuned to have their lowest unoccupied molecular orbital (LUMO) close to the anchoring group and the TiO₂ surface and their highest occupied molecular orbital (HOMO) located further away from the semiconductor surface.⁸ These dyes therefore show intramolecular charge transfer (ICT) from the donor to the acceptor upon excitation.

A variation of the standard n-type DSCs using an n-type semiconductor are p-type DSCs, which use a p-type semiconductor (NiO) as a photocathode.⁹ For these DSCs, so-called p-type dyes have been designed where the donor is located close to the anchoring group of the molecule and the acceptor is located far away from the anchoring group.^{10,11} As a consequence, these dyes show intramolecular charge transfer in the opposite direction to n-type dyes.

The different reactions in the DSC are spread over a wide range of time scales: from femtoseconds for electron injection to the tens of milliseconds for recombination of injected

[†] Uppsala University.

[‡] BASF SE.

- (1) O'Regan, B.; Grätzel, M. *Nature* **1991**, *353*, 737–740.
- (2) Hagfeldt, A.; Grätzel, M. *Acc. Chem. Res.* **2000**, *33*, 269–277.
- (3) Grätzel, M. *J. Photochem. Photobiol., A* **2004**, *164*, 3–14.
- (4) Peter, L. M. *J. Phys. Chem. C* **2007**, *111*, 6601–6612.
- (5) Bach, U.; Lupo, D.; Comte, P.; Moser, J. E.; Weissörtel, F.; Salbeck, J.; Spreitzer, H.; Grätzel, M. *Nature* **1998**, *395*, 583–585.
- (6) Yum, J. H.; Chen, P.; Grätzel, M.; Nazeeruddin, M. K. *ChemSusChem* **2008**, *1*, 699–707.

- (7) Nazeeruddin, M. K.; Kay, A.; Rodicio, I.; Humphry-Baker, R.; Müller, E.; Liska, P.; Vlachopoulos, N.; Grätzel, M. *J. Am. Chem. Soc.* **1993**, *115*, 6382–6390.
- (8) Mishra, A.; Fischer, M. K. R.; Bäuerle, P. *Angew. Chem., Int. Ed.* **2009**, *48*, 2474–2499.
- (9) He, J. J.; Lindstrom, H.; Hagfeldt, A.; Lindquist, S. E. *J. Phys. Chem. B* **1999**, *103*, 8940–8943.
- (10) Qin, P.; Zhu, H. J.; Edvinsson, T.; Boschloo, G.; Hagfeldt, A.; Sun, L. C. *J. Am. Chem. Soc.* **2008**, *130*, 8570–8571.
- (11) Qin, P.; Wiberg, J.; Gibson, E. A.; Linder, M.; Li, L.; Brinck, T.; Hagfeldt, A.; Albinsson, B.; Sun, L. *J. Phys. Chem. C* **2010**, *114*, 4738–4748.

electrons with acceptors in the electrolyte. Many of these reactions have been studied by transient absorption spectroscopy using pulsed lasers to excite the sample.^{12–14} Here, we use photoinduced absorption (PIA) spectroscopy, where the difference in absorption of a sample with and without excitation is measured on a relatively long time scale, typically tens of milliseconds.^{15,16}

Recently, several cases were reported where transient absorption signals apparently due to ground-state bleaching of dye molecules did not disappear after dye molecules had been regenerated: Meyer et al. assigned a “peak-bleach” feature, which vanished with a rate slower than dye regeneration, to slow cation transfer.¹⁷ We observed a blue shift of dye absorption upon electron accumulation in the TiO₂, which we attributed to electrons affecting the LUMO of the sensitizer.¹⁸ Snaith et al. interpreted an apparent ground-state bleach of the indoline dye, D149, in the presence of spiro-MeOTAD as evidence of long-lived photoreduced sensitizers.¹⁹ O’Regan et al. found a bleach correlated to electron extraction from TiO₂ rather than to regeneration of oxidized dye molecules.²⁰

We consider here whether local electric fields acting on ground-state dye molecules can provide a better explanation for the observed signals. Such electric fields could lead to a change in the absorption spectrum due to the Stark effect (also called electrochromism or electroabsorption).^{21–23} The change in transition frequency ($\Delta\nu$) due to an external electric field (\vec{E}) is given by²³

$$\Delta\nu = -\Delta\vec{\mu} \cdot \vec{E} - \frac{1}{2}\vec{E} \cdot \underline{\Delta\alpha} \cdot \vec{E} \quad (1)$$

where $\Delta\vec{\mu}$ is the change in dipole moment and $\underline{\Delta\alpha}$ is the change in polarizability between the ground and excited state of the molecule. From eq 1, one distinguishes first- and second-order Stark effects, which are, respectively, linear and quadratic in the electric field. Stark (electroabsorption) spectroscopy has been used to determine $\Delta\mu$ and $\Delta\alpha$ from disordered samples, where only the second-order effect is observed,^{23–25} and in some cases from ordered Langmuir–Blodgett films, where both the first- and second-order effect can be observed.^{26,27} In the latter case, the change in absorbance ($\Delta A = A(\nu, E_z) - A(\nu, E_z = 0)$)

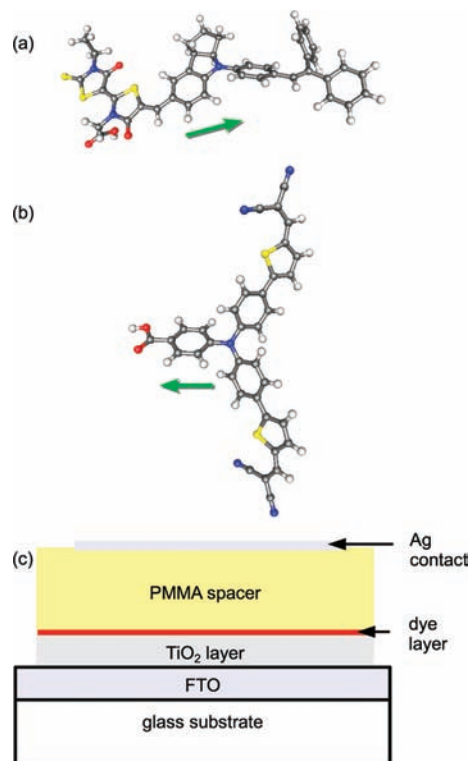


Figure 1. Chemical structures of D149 (a) and P1 (b) with the direction of the difference in dipole moment between ground and excited states ($\Delta\mu$) obtained from TD-DFT calculations indicated by green arrows. By definition, $\vec{\mu}$ points from negative to positive charge. (c) Schematic diagram of devices used to measure electroabsorption.

when the field is applied normal to the substrate (in the z direction) can be obtained from a Taylor expansion of A around ν at $E_z = 0$ (derivation in Supporting Information). The terms of this expansion linear and quadratic with the electric field are given by

$$\Delta A = -\frac{dA}{d\nu} \Delta\mu_z E_z + \frac{1}{2} \left(\frac{d^2 A}{d\nu^2} \Delta\mu_z^2 - \frac{dA}{d\nu} \Delta\alpha \right) E_z^2 \quad (2)$$

It is this directional effect that is of interest here, and we thus need samples, in which dye molecules are ordered, to test our hypothesis. We used two organic dyes with intramolecular charge transfer upon excitation for our experiments: the indoline sensitizer, D149 (Figure 1a), which has given high efficiencies in liquid electrolyte DSCs,^{28,29} as well as the p-type sensitizer, P1 (Figure 1b).¹⁰ Intramolecular charge transfer should occur in opposite directions relative to the anchoring group for these two dyes, and thus, the component of $\Delta\vec{\mu}$ normal to the TiO₂ surface should be pointing in opposite directions and Stark shifts would be expected to have opposite signs for the two sensitizer. To orientate the molecules for electroabsorption measurements, they were adsorbed to flat TiO₂ films (Figure 1c).

In the following, we present a method for sample preparation and measurements of electroabsorption spectra and hence the Stark shift of dye monolayers attached to flat TiO₂ substrates. By comparing these spectra, calculated spectra, and spectra of

- (12) O’Regan, B.; Moser, J.; Anderson, M.; Grätzel, M. *J. Phys. Chem.* **1990**, *94*, 8720–8726.
 (13) Eichberger, R.; Willig, F. *Chem. Phys.* **1990**, *141*, 159–173.
 (14) Tachibana, Y.; Moser, J. E.; Grätzel, M.; Klug, D. R.; Durrant, J. R. *J. Phys. Chem.* **1996**, *100*, 20056–20062.
 (15) Boschloo, G.; Hagfeldt, A. *Chem. Phys. Lett.* **2003**, *370*, 381–386.
 (16) Boschloo, G.; Hagfeldt, A. *Inorg. Chim. Acta* **2008**, *361*, 729–734.
 (17) Staniszewski, A.; Ardo, S.; Sun, Y.; Castellano, F. N.; Meyer, G. J. *J. Am. Chem. Soc.* **2008**, *130*, 11586–11587.
 (18) Cappel, U. B.; Gibson, E. A.; Hagfeldt, A.; Boschloo, G. *J. Phys. Chem. C* **2009**, *113*, 6275–6281.
 (19) Snaith, H. J.; Petrozza, A.; Ito, S.; Miura, H.; Grätzel, M. *Adv. Funct. Mater.* **2009**, *19*, 1810–1818.
 (20) Anderson, A. Y.; Barnes, P. R. F.; Durrant, J. R.; O’Regan, B. C. J. *J. Phys. Chem. C* **2010**, *114*, 1953–1958.
 (21) Stark, J. *Nature* **1914**, *92*, 401–401.
 (22) Leone, M.; Paoletti, A.; Robotti, N. *Phys. Perspect.* **2004**, *6*, 271–294.
 (23) Bubblitz, G. U.; Boxer, S. G. *Annu. Rev. Phys. Chem.* **1997**, *48*, 213–242.
 (24) Boxer, S. G. *J. Phys. Chem. B* **2009**, *113*, 2972–2983.
 (25) Vance, F. W.; Williams, R. D.; Hupp, J. T. *Int. Rev. Phys. Chem.* **1998**, *17*, 307–329.
 (26) Bücher, H.; Wiegand, J.; Snavely, B. B.; Beck, K. H.; Kuhn, H. *Chem. Phys. Lett.* **1969**, *3*, 508–511.
 (27) Ohta, N.; Okazaki, S.; Yamazaki, I. *Chem. Phys. Lett.* **1994**, *229*, 394–400.

- (28) Horiuchi, T.; Miura, H.; Sumioka, K.; Uchida, S. *J. Am. Chem. Soc.* **2004**, *126*, 12218–12219.
 (29) Ito, S.; Zakeeruddin, S. M.; Humphry-Baker, R.; Liska, P.; Charvet, R.; Comte, P.; Nazeeruddin, M. K.; Pechy, P.; Takata, M.; Miura, H.; Uchida, S.; Grätzel, M. *Adv. Mater.* **2006**, *18*, 1202–1205.

electrochemically oxidized dye molecules with photoinduced absorption spectra of the dye molecules adsorbed to mesoporous TiO₂, we provide evidence for the presence of local electric fields acting on the dye molecules under solar cell working conditions.

Experimental Methods

Samples to measure the Stark effect directly, which we will refer to as electroabsorption samples, are shown in a schematic diagram in Figure 1c. The samples were fabricated on FTO substrates. Flat anatase TiO₂ layers were prepared on the substrates by spray pyrolysis. The films were heated to 450 °C and then immersed for 10 min in dye solution. For D149, the dye bath contained 0.5 mM D149 (obtained from ABCR) in a 1:1 mixture of acetonitrile and *tert*-butanol. For P1 (available from previous studies¹⁰), the dye bath consisted of 0.1 mM P1 in ethanol. The films were washed in ethanol after dye dipping to remove excess nonbound dye molecules. Poly(methyl methacrylate) (PMMA) (Aldrich, $M_w = 15\,000$) was applied by spin-coating from a 1:20 mixture (with respect to weight) of PMMA and dichloromethane (DCM) for 15 s at 2000 rpm. The PMMA layer was 770 ± 50 nm thick for the D149 sample and 620 ± 50 nm for the P1 sample. Thicknesses were measured on a Dektak 150 surface profiler from Veeco. Silver contacts of a few nanometers thickness were evaporated using a Leica EM MED020 evaporator. This sample preparation provides an ordered monolayer of dye molecules within a parallel plate capacitor where the FTO and the silver act as the capacitor plates.

Samples for UV–visible absorption, photoinduced absorption, and spectroelectrochemical measurements were prepared by doctor blading a colloidal TiO₂ paste (Dyesol, DSL 18NR-T), diluted 40:60 with respect to weight with terpineol on FTO substrates, resulting in a final film thickness of $\sim 2\ \mu\text{m}$. The films were sintered for 1 h at 450 °C and then dyed for 16 h in the above-mentioned dye solutions of D149 and P1. The electrolyte used in PIA measurements consisted of 0.5 M tetrabutylammonium (TBA) iodide and 0.05 M I₂ in methoxypropionitrile (MPN).

Electroabsorption measurements (direct measurements of the Stark effect) and photoinduced absorption measurements were performed on the same setup. White probe light was provided by a 20 W tungsten-halogen lamp. For electroabsorption measurements, a voltage was modulated across the sample using a function generator (HP 33120A), while, for PIA measurements, the same frequency generator was used to square-wave modulate (on/off) a blue LED (Luxeon Star, 1 W, Royal Blue, 460 nm). The LED light was superimposed with the white light at the sample and used for excitation. The probe light transmitted through the samples was focused onto a monochromator (Acton Research Corporation SP-150) and detected by a UV enhanced silicon photodiode connected to a current amplifier and lock-in amplifier (Stanford Research Systems models SR570 and SR830, respectively). This setup enables us to measure small changes in the absorbance of the samples (on the order of 10^{-6}). The intensity of the probe light on the sample was approximately 1/8 sun, and for PIA measurements, the intensity of the LED at the sample was approximately 24 mW cm⁻². For Stark effect measurements, the modulation frequency of the voltage was 93 Hz and ΔA was calculated from the change in transmission in phase with the modulation. For PIA measurements, the modulation frequency was 9.3 Hz (3 Hz for P1 with electrolyte) and ΔA was calculated from the in-phase and out-of-phase parts of the change in transmission.

UV–visible spectra were recorded on an HR-2000 Ocean Optics fiber optics spectrophotometer. Electrochemical measurements were performed on a CH Instruments 660 potentiostat with a three-electrode setup. For the oxidation of D149, cyclic voltammetry was performed using a dye-coated mesoporous TiO₂ film on an FTO substrate as the working electrode, a platinum wire as the counter electrode, and a Ag electrode as pseudo reference electrode. The electrolyte solution was 0.1 M TBAClO₄ in MPN. The setup was

internally calibrated with ferrocene/ferrocenium (Fc/Fc⁺) using a platinum working electrode. UV–visible spectra were measured during cyclic voltammetry.

All calculations were carried out with the TURBOMOLE suite of programs.³⁰ Geometries were optimized at the BP86/def-SV(P) level.^{31–33} The dye molecules were then reoriented by suitable coordinate transformations such that

1. for D149, the long molecular axis (by moments of inertia) is along the z -axis with the anchor to the positive end, and
2. for P1, the anchor group lies on the z -axis and also oriented to the positive end, which also forms the C2 symmetry axis of the molecule.

These orientations are chosen to mirror the situation of the dyes attached to TiO₂, with the z -axis approximating the normal to the surface plane. Single-point calculations were carried out at the BLYP/def-TZVP level^{34–36} with and without an electric field applied. The field strength and orientation were ($x = 0, y = 0, z = 5.0 \times 10^8$) V m⁻¹. This results in the negative pole of the electric field being on the anchoring group side of the molecules for both P1 and D149. The excited states are calculated by the time-dependent density functional formalism at the same level of theory.^{37,38} Ground and excited state dipole moments were calculated from the (un)polarized ground state and excited state densities, respectively.³⁹

Results and Discussions

The direction of change in dipole moment between the ground and excited state as calculated by TD-DFT is shown in Figure 1a,b for D149 and P1, confirming that ICT relative to the anchoring group occurs indeed in opposite directions for the two sensitizers. The magnitude of the change in the dipole moment ($|\Delta\vec{\mu}|$) was 7.1 D for D149 and 3.3 D for P1. Howie et al.⁴⁰ calculated possible orientations of D149 on the TiO₂ surface: In the case of bidentate binding, the molecule is expected to be lying down on the surface while, in the case of monodentate binding, the molecule is expected to stand up on the surface. In the latter case, $\Delta\mu_z$ is expected to be almost equal to $|\Delta\vec{\mu}|$, while, in the former case, it is expected to be much smaller.

Electroabsorption spectra of D149 and P1 measured on samples as presented in Figure 1c are shown in Figure 2a. The spectra were measured with a modulation voltage (V_{mod}) of 20 V, corresponding to an electric field strength of approximately 2.6×10^7 V m⁻¹ for D149 and 3.2×10^7 V m⁻¹ for P1, and the negative pole on the FTO (representing where the negative pole in the solar cell would be). For D149, the spectrum shows an increase in absorption at the blue edge and a decrease in absorption at the red edge of the spectrum. For P1, this effect is reversed. In accordance with these observations, TD-DFT calculations showed a blue-shifted absorption wavelength for

(30) Ahlrichs, R.; Bär, M.; Häser, M.; Horn, H.; Kölmel, C. *Chem. Phys. Lett.* **1989**, *162*, 165–169.

(31) Becke, A. D. *Phys. Rev. A* **1988**, *38*, 3098–3100.

(32) Perdew, J. P. *Phys. Rev. B* **1986**, *33*, 8822–8824.

(33) Schäfer, A.; Horn, H.; Ahlrichs, R. *J. Chem. Phys.* **1992**, *97*, 2571–2577.

(34) Becke, A. D. *J. Chem. Phys.* **1993**, *98*, 1372–1377.

(35) Lee, C. T.; Yang, W. T.; Parr, R. G. *Phys. Rev. B* **1988**, *37*, 785–789.

(36) Schäfer, A.; Huber, C.; Ahlrichs, R. *J. Chem. Phys.* **1994**, *100*, 5829–5835.

(37) Bauernschmitt, R.; Ahlrichs, R. *Chem. Phys. Lett.* **1996**, *256*, 454–464.

(38) Bauernschmitt, R.; Häser, M.; Treutler, O.; Ahlrichs, R. *Chem. Phys. Lett.* **1997**, *264*, 573–578.

(39) Furche, F.; Ahlrichs, R. *J. Chem. Phys.* **2002**, *117*, 7433–7447.

(40) Howie, W. H.; Claeysens, F.; Miura, H.; Peter, L. M. *J. Am. Chem. Soc.* **2008**, *130*, 1367–1375.

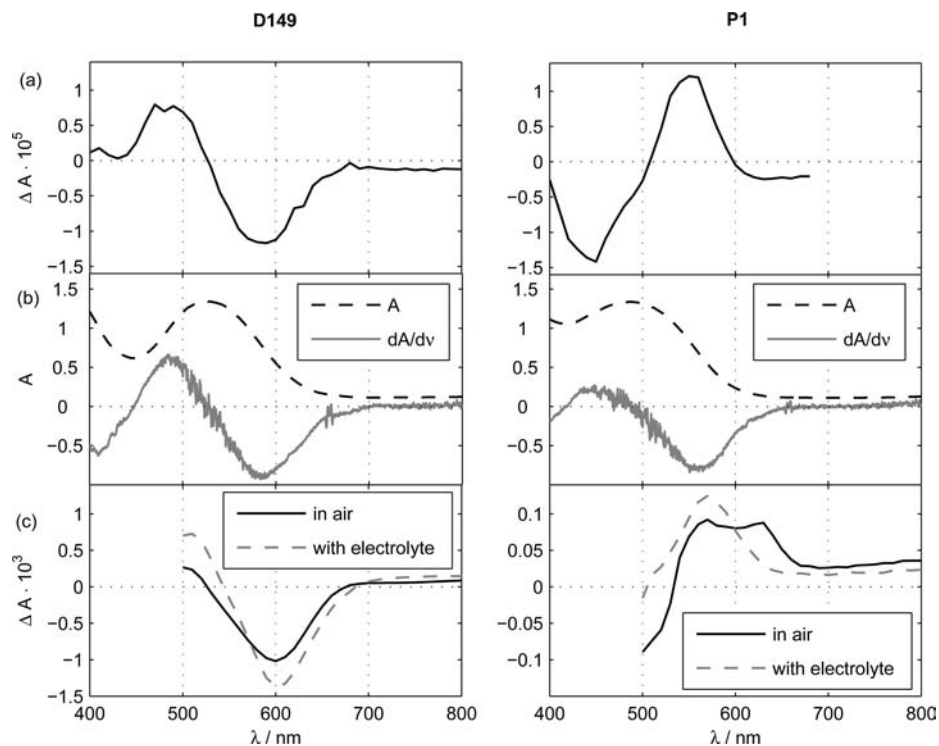


Figure 2. (a) Electroabsorption spectra of D149 (left) and P1 (right). (b) Absorption spectra (A) of D149 and P1 on mesoporous TiO_2 and first derivatives of absorption spectra ($(dA)/(dv)$) multiplied by $-5 \times 10^{13} \text{ s}^{-1}$. (c) PIA spectra of D149 and P1 on mesoporous TiO_2 in air and in presence of redox electrolyte.

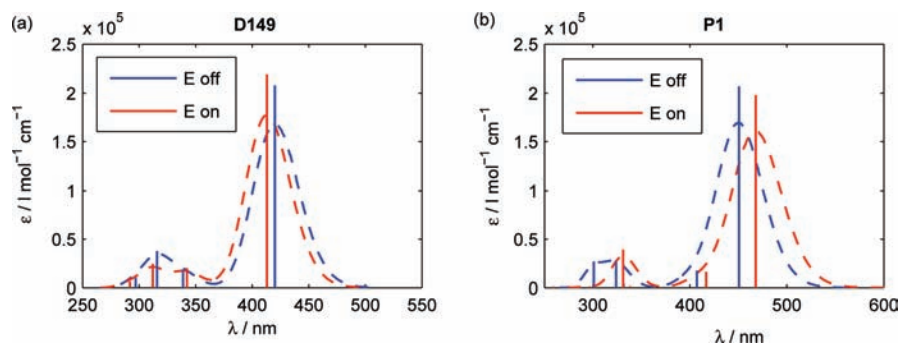


Figure 3. Calculated absorption spectra. Electronic transitions of D149 (a) and P1 (b) calculated by TD-DFT in absence and in presence of an electric field with a field strength of $E = 5 \times 10^8 \text{ V m}^{-1}$. Dashed lines indicate simulated absorption spectra obtained by Gaussian broadening of the transition lines.

D149 and a red-shifted absorption for P1, when a corresponding external electric field was applied in the computation (Figure 3). Additionally, we were able to measure similar effects with other organic dyes used in DSCs such as triphenylamine based dyes designed for the n-type DSC^{41,42} and for perylenes.⁴³

Absorption spectra of D149 and P1 on mesoporous TiO_2 films and the first derivatives of these spectra with respect to frequency are shown in Figure 2b. The absorbance of the dyes anchored to flat TiO_2 substrates is too low to be determined accurately by transmission measurements, but we estimated the absorbance maximum of D149 on a flat film to be 2.2×10^{-3}

(method described in Supporting Information). This corresponds to a surface coverage of $3.2 \times 10^{-11} \text{ mol cm}^{-2}$, which is approximately half of the value reported by Howie et al.⁴⁰ It can be seen that the shape of the electroabsorption spectra correlates with the first derivatives of the absorption spectra with respect to frequency in agreement with eq 2. We tested the effect of changing the modulation voltage on the spectra and found that the amplitude of the signal increased linearly with V_{mod} (Figure 4). This proves that the measured effect is linear in the electric field and hence that we measured the first-order Stark effect. Therefore, we could neglect terms of higher E dependence and use the first term in eq 2 to estimate $\Delta\mu_z$. For D149, comparing the derivative of A to ΔA gave $\Delta\mu_z \approx 1 \text{ D}$ (for details of the calculation see Supporting Information). This value is smaller than $\Delta\vec{\mu}$ obtained from TD-DFT calculations but still the same order of magnitude. This might indicate that D149 is orientated almost parallel to the surface and prefers bidentate binding, which according to calculations is the more

(41) Hagberg, D. P.; Edvinsson, T.; Marinado, T.; Boschloo, G.; Hagfeldt, A.; Sun, L. C. *Chem. Commun.* **2006**, 2245–2247.

(42) Hagberg, D. P.; Jiang, X.; Gabrielsson, E.; Linder, M.; Marinado, T.; Brinck, T.; Hagfeldt, A.; Sun, L. C. *J. Mater. Chem.* **2009**, *19*, 7232–7238.

(43) Cappel, U. B.; Karlsson, M. H.; Pschirer, N. G.; Eickemeyer, F.; Schöneboom, J.; Erk, P.; Boschloo, G.; Hagfeldt, A. *J. Phys. Chem. C* **2009**, *113*, 14595–14597.

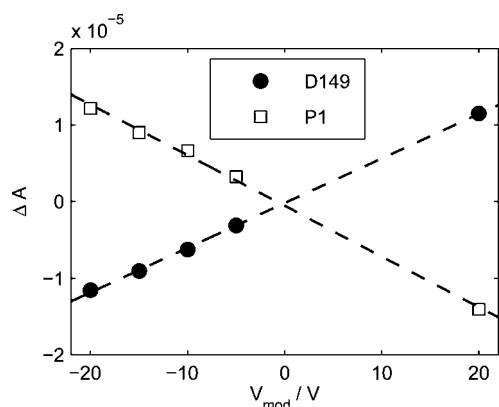


Figure 4. Electroabsorption in dependence of modulation voltage at 580 nm for D149 and at 550 nm for P1. Dashed lines indicate a linear fit to the data.

stable form of binding.⁴⁰ However, the lower experimental value could also be due to the fact that the TiO₂ surface is not completely flat. This leads to not all molecules pointing in the same direction and therefore to a lowering of $\Delta\mu_z$. Determinations of $|\Delta\vec{\mu}|$ for dyes adsorbed to TiO₂ nanoparticles have been previously carried out in randomly orientated samples by measuring the second-order Stark effect.^{44–47} Stark emission spectroscopy⁴⁴ and electroabsorption spectroscopy^{45–47} were used to study whether electron injection occurs via a direct charge-transfer transition from the dye to the nanoparticle based on the formation of a charge-transfer complex between the dye and the semiconductor. In our case, $\Delta\mu_z$ is a measure of the internal charge transfer of the sensitizing dye toward the TiO₂ surface.

We compared the electroabsorption spectra to PIA spectra obtained for D149 and P1 attached to mesoporous TiO₂ in air and in the presence of a redox electrolyte containing TBAI and I₂ (Figure 2c). Both PIA spectra of D149 look remarkably similar to the electroabsorption spectra. In the absence of electrolyte, the transient species present upon excitation should be electrons in the TiO₂ and oxidized D149. To assign features to these species, separate measurements of the spectra of oxidized dye molecules by spectroelectrochemistry are useful.¹⁸ To obtain these, we performed cyclic voltammetry on a mesoporous TiO₂ film dyed in D149 (cyclic voltammogram of D149 in the Supporting Information). The change in absorbance of D149 during oxidation is shown in Figure 5. Features due to the absorbance of the oxidized dye can be seen in the near-infrared (NIR) part of the spectrum (Figure 5a). Interestingly, some spectral changes occur in the dye spectrum prior to the start of the oxidation process (Figure 5b). During this time, a small current flows in cyclic voltammetry due to the discharging of the porous TiO₂ electrode. The absorption spectrum of D149 is red-shifted during this discharge. Presumably, some trapped electrons are removed from the TiO₂ prior to the oxidation of D149, giving the TiO₂ a more positive charge and inducing a Stark shift in D149. A similar result was obtained for P1, where the dye was blue-shifted prior to the onset of oxidation (Supporting Information).

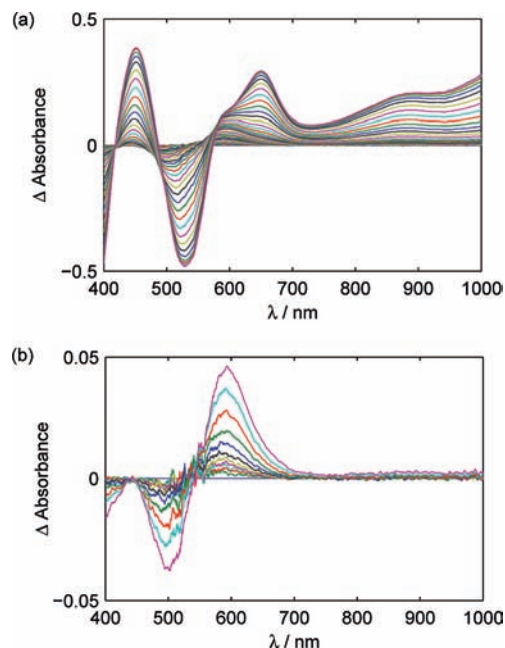


Figure 5. Change in absorption of D149 during oxidation by cyclic voltammetry. (a) Spectra measured during the entire oxidation process showing the increase in absorption of oxidized D149 compared to absorption of ground-state molecules. (b) Spectra measured before the onset of oxidation of D149 showing the Stark shift of D149.

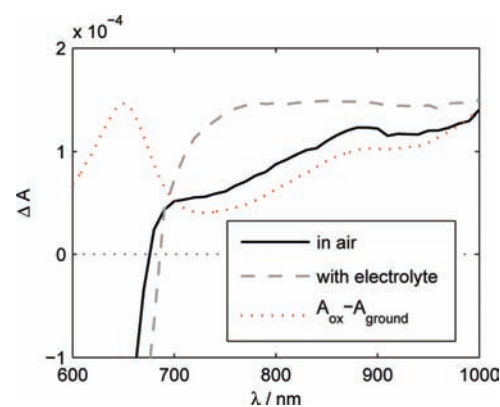


Figure 6. PIA spectra of D149 on TiO₂ at air and in presence of redox electrolyte compared to the difference in absorption of electrochemically oxidized D149 and ground-state D149 ($A_{\text{ox}} - A_{\text{ground}}$). The latter spectrum was scaled by 5×10^{-4} to match the amplitude of the PIA spectra in the NIR.

Comparison of the PIA spectrum with the spectrum of electrochemically oxidized D149 shows that absorption features of the oxidized dye are present in the NIR part of the PIA spectrum (Figure 6). These features vanish upon addition of redox electrolyte and are replaced by the broad absorption of electrons in the TiO₂ in the NIR, indicating that the dye is successfully regenerated by the redox electrolyte (Figure 6). However, the PIA spectrum is dominated by the Stark signal which has a 10 times larger amplitude than absorption signals due to oxidized dye molecules or due to electrons in the TiO₂.

The PIA spectrum of P1 on TiO₂ in air shows peaks at 560 and 630 nm (Figure 2c). The peak at 630 nm corresponds to the peak of oxidized P1 (confirmed in separate spectroelectrochemical measurements, see Supporting Information), indicating that the dye has injected electrons into TiO₂ upon excitation, while the peak at 560 nm corresponds to the Stark signal of P1. Upon addition of redox electrolyte, the peak of the oxidized

(44) Walters, K. A.; Gaal, D. A.; Hupp, J. T. *J. Phys. Chem. B* **2002**, *106*, 5139–5142.

(45) Khoudiakov, M.; Parise, A. R.; Brunschwig, B. S. *J. Am. Chem. Soc.* **2003**, *125*, 4637–4642.

(46) Nawrocka, A.; Krawczyk, S. *J. Phys. Chem. C* **2008**, *112*, 10233–10241.

(47) Nawrocka, A.; Zdyb, A.; Krawczyk, S. *Chem. Phys. Lett.* **2009**, *475*, 272–276.

dye at 630 nm disappears indicating efficient dye regeneration while the peak at 560 nm remains.

Therefore, for both dyes, there are local electric fields acting on the dye molecules in the absence as well as in the presence of redox electrolyte leading to the observation of Stark signals in the PIA spectra. The occurrence of Stark shifts in dye-sensitized TiO₂ electrodes in air may be explained by the electric field that will exist between the positive charge on the oxidized dye and the injected electron in the TiO₂ particle and its effect on the neighboring dye molecules in the ground state. In the presence of a concentrated electrolyte, electric fields are only expected to be present in the Helmholtz layer. Our findings imply therefore that the dye molecules are located within this region. We obtained a similar result with a redox electrolyte containing lithium iodide and iodine (Supporting Information), where the cation is much smaller and more likely to adsorb closely to the TiO₂ surface. The conclusion that the dye must be mostly inside the ionic double layer at the electrode/electrolyte interface was drawn earlier by Zaban et al., who found that the redox potential for a number of sensitizers adsorbed onto TiO₂ is pH-dependent, in contrast their redox potentials in solution.^{48,49} They proposed that the location of dye, mostly inside the ionic double layer made their redox potential follow changes in band edge potentials of the semiconductor.⁴⁹

By comparing the magnitudes of the transient and steady state absorption signals from the electroabsorption and PIA measurements, the change in potential drop across the dye was estimated to be at least 6 mV in the PIA experiment with TBAI electrolyte. From the NIR absorption of electrons in the TiO₂ in the PIA measurement, the concentration of electrons in the mesoporous TiO₂ electrode and hence the photoinduced charge could be calculated: $1.2 \times 10^{-5} \text{ C cm}^{-2}$. Using this value, we estimated the capacity of the Helmholtz double layer capacitor to be $4 \mu\text{F cm}^{-2}$ for a flat TiO₂ electrode, which is a reasonable value. For P1, a charge of $1.8 \times 10^{-6} \text{ C cm}^{-2}$ and a Helmholtz capacity of $6 \mu\text{F cm}^{-2}$ were obtained. Details of these calculations are presented in the Supporting Information.

The increased potential drop in the Helmholtz layer implies that the conduction band edge of TiO₂ is shifted toward a negative potential upon photoinduced charge injection and/or that the redox potential of the electrolyte is shifted to a positive potential. Thus far, such shifts have been mostly neglected in DSC research. In principle, addition of electrons into the undoped mesoporous TiO₂ electrode should always be accompanied by charge compensation through ions in the elec-

trolyte. This will lead to charging of the Helmholtz capacitor and a shift of the conduction band, unless the surface charge of TiO₂ is changed by specific adsorption or desorption of ions. Very recently, it was shown that illumination of a DSC under open-circuit conditions is accompanied by a small positive shift ($\sim 1 \text{ mV}$) of the redox potential of I^-/I_3^- .⁵⁰ This also leads to an increased voltage drop across the Helmholtz layer. Here, we have demonstrated that conduction band and/or redox potential shifts are occurring in DSCs upon illumination. Using PIA along with electroabsorption spectroscopy, we now have a tool to investigate such shifts in DSCs.

Conclusions

In conclusion, we have shown that a potential drop across dye molecules upon electron injection into TiO₂ leads to a Stark shift of the absorption spectra of the dye. It is vital to consider these shifts when analyzing transient absorption data of DSCs, as they can be much higher in intensity than features due to the absorbance of transient species. Additionally, electroabsorption spectroscopy of dye molecules anchored to flat TiO₂ substrates can be used to determine the direction and magnitude of $\Delta\vec{\mu}$ with respect to the semiconductor surface for dyes used in DSCs. We have shown that the direction of $\Delta\vec{\mu}$ relative to the TiO₂ surface for the n-type dye D149 is opposite to that for the p-type dye P1, as was intended by dye design and predicted by calculations. Therefore, electroabsorption spectroscopy provides a method to determine the effectiveness of the internal charge transfer of dye molecules under solar cell conditions. If accurate determinations of the absorbance of samples used to measure the Stark effect can be made, it will become possible to determine accurately the magnitude of $\Delta\vec{\mu}$ normal to the semiconductor surfaces and from this infer the orientation of the dye molecules. The occurrence of Stark shifts in sensitizer molecules in DSCs gives evidence that the electrical field across the dye changes upon illumination, which must be caused by a band edge shift of the TiO₂ semiconductor in these devices and/or a shift of the redox potential of the electrolyte.

Acknowledgment. The authors thank Henry Snaith (Oxford University) and Felix Eickemeyer (BASF SE) for discussions and Peng Qin (KTH, Stockholm) and Licheng Sun (KTH, Stockholm) for the provision of P1. We acknowledge the financial support of the Bundesministerium für Bildung und Forschung (BMBF), the BASF SE and the Swedish Energy Agency.

Supporting Information Available: Derivation of eq 2; estimation of the absorbance of D149 in electroabsorption samples; spectroelectrochemistry of P1; additional PIA spectra and calculations of $\Delta\mu_z$, of the potential drop and of Helmholtz capacities. This material is available free of charge via the Internet at <http://pubs.acs.org>.

JA102334H

(48) Zaban, A.; Ferrere, S.; Sprague, J.; Gregg, B. A. *J. Phys. Chem. B* **1997**, *101*, 55–57.

(49) Zaban, A.; Ferrere, S.; Gregg, B. A. *J. Phys. Chem. B* **1998**, *102*, 452–460.

(50) Dor, S.; Grinis, L.; Ruhle, S.; Zaban, A. *J. Phys. Chem. C* **2009**, *113*, 2022–2027.